Available online at www.sciencedirect.com
ScienceDirect
Trans. Nonferrous Met. Soc. China 35(2025) 313−325
Transactions of Nonferrous Metals Society of China
www.tnmsc.cn

Flotation separation of chalcopyrite from pyrite using mineral fulvic acid as selective depressant under weakly alkaline conditions

Zhi-hao SHEN, Shu-ming WEN, Jia-mei HAO, Qi-cheng FENG

State Key Laboratory of Complex Nonferrous Metal Resources Clean Utilization,
Faculty of Land Resource Engineering, Kunming University of Science and Technology, Kunming 650093, China

Received 2 May 2023; accepted 20 December 2023

Abstract: Mineral fulvic acid (MFA) was used as an eco-friendly pyrite depressant to recover chalcopyrite by flotation with the use of the butyl xanthate as a collector. Flotation experiments showed that MFA produced a stronger inhibition effect on pyrite than on chalcopyrite. The separation of chalcopyrite from pyrite was realized by introducing 150 mg/L MFA at a pulp pH of approximately 8.0. The copper grade, copper recovery, and separation efficiency were 28.03%, 84.79%, and 71.66%, respectively. Surface adsorption tests, zeta potential determinations, and localized electrochemical impedance spectroscopy tests showed that more MFA adsorbed on pyrite than on chalcopyrite, which weakened the subsequent interactions between pyrite and the collector. Atomic force microscope imaging further confirmed the adsorption of MFA on pyrite, and X-ray photoelectron spectroscopy results indicated that hydrophilic Fe-based species on the pyrite surfaces increased after exposure of pyrite to MFA, thereby decreasing the floatability of pyrite.
Key words: mineral fulvic acid; chalcopyrite; pyrite; flotation separation

1 Introduction

Copper is an irreplaceable element in the economic and technological development of modern society [1−4]. Copper is mainly extracted from copper−sulfide mineral resources that are easily beneficiated. Among such minerals, chalcopyrite ($CuFeS_2$) is a Cu-bearing sulfide mineral that has attracted growing research attention owing to its high recoverability in the context of ever-dwindling copper resources [5−8]. In general, chalcopyrite can be effectively recovered using the froth flotation method before metallurgical treatments [9−11]. Unfortunately, poor industrial indexes are frequently obtained because of the presence of associated gangue minerals, especially pyrite (FeS_2), a representative metallic sulfide mineral that is ubiquitously distributed over the earth [12−15]. Accordingly, there is an urgent need for depressants for pyrite.

Conventionally, inorganic reagents, such as calcium oxide and sodium cyanide, are commonly used as industrial depressants to inhibit pyrite when recovering chalcopyrite by flotation [16−19]. However, the use of these two reagents usually results in a toxic and highly alkalinized flotation pulp. This feature not only affects the flotation of other target minerals, but also leads to a loss of flotation devices through alkaline corrosion. Most importantly, such by-products seriously threaten the physical health of operating workers and the security of the environment [19,20]. Environmentally friendly depressants for pyrite used in weak-alkalinity flotation systems therefore have therefore drawn considerable research interest [21].

Starch, polyacrylamide, carboxymethyl cellulose, lignosulfonate, and chitosan are traditional macro-

Corresponding author: Qi-cheng FENG, Tel: +86-15987190563, E−mail: fqckmust@163.com
https://doi.org/10.1016/S1003-6326(24)66681-1

molecular organic depressants for pyrite [22−25]. Additionally, several studies have reported on the use of novel organic depressants to depress pyrite. HAN et al [18,26,27] reported that salicylic acid, lactic acid, and pyrogenic acid all exhibited a stronger inhibition effect on pyrite than on chalcopyrite. Adsorption tests suggested that hydrophilic functional groups in these depressants selectively adsorbed on the surfaces of pyrite, thereby depressing the flotation of pyrite. LIU et al [28] found that konjac glucomannan depressed pyrite more efficiently than dextrin, starch, and guar gum, where the flotation separation between pyrite and chalcopyrite was realized by adding 10 mg/L of konjac glucomannan. Analysis of these results indicated that hydrogen bonding and acid-base interactions might play a crucial role in depressing pyrite by konjac glucomannan. KHOSO et al [7] efficiently separated chalcopyrite from pyrite through the use of a new environmentally friendly depressant, poly-glutamic acid (PGA). Analyses showed that hydrophilic species were generated on the surfaces of pyrite after exposure to PGA, thus attenuating its hydrophobicity. BAI et al [29,30] revealed that sodium dimethyl dithiocarbamate (SDD), an organic reagent having excellent chelating ability for heavy metal ions, markedly inhibited pyrite whereas chalcopyrite was basically unaffected. The recovery of chalcopyrite was achieved following addition of low dosages of SDD in flotation testing of artificially mixed minerals. Intriguingly, pyrite exploited from different ore deposits exhibits different flotation behavior, owing to the crystal defects and structural inhomogeneity of pyrite. These variations contribute to ongoing difficulties in separating pyrite from chalcopyrite and other target minerals [7,31,32]. Therefore, a reasonable and alternative depressant for pyrite would have implications for both theoretical research and industrial production.

Fulvic acid is a heterogeneous and amorphous aliphatic−aromatic organic acid compound, which is commonly formed by the decomposition and synthesis of micro-organisms from plant residues. It has a rich variety of activated functional groups, e.g., carboxyl, carbonyl, and phenol hydroxyl groups [33,34]. Fulvic acid is widely used in in pharmaceuticals, agriculture, husbandry, and other fields owing to its high aqueous solubility and physiological activity [33,34]. However, the use of fulvic acid to separate minerals has rarely been reported. Accordingly, in the present study, mineral fulvic acid (MFA), a kind of fulvic acid extracted from organic mineral substances including lignite, peat, and weathered coal, was used as a pyrite depressant to recover chalcopyrite by flotation. The inhibition mechanism of MFA on pyrite was investigated through the use of multiple characterization methods. The aim of this study was to report a novel and eco-friendly pyrite depressant for effectively recovering chalcopyrite in flotation.

2 Experimental

2.1 Materials

Pyrite and chalcopyrite specimens were sourced from Kunming, Yunnan Province, China. Raw mineral blocks were smashed, milled, and sifted. Powdered products with particle diameters in the range of 38−75 μm were collected for micro-flotation and surface adsorption tests. Samples having a diameter of less than 38 μm were used for zeta potential determinations and X-ray photo-electron spectroscopy (XPS) tests. Additionally, mineral flakes were used in atomic force micro-scope (AFM) observations and localized electro-chemical impedance spectroscopy (LEIS) tests. The X-ray diffraction (XRD) patterns (Fig. 1) and multi-element detection results (Table 1) showed that both minerals had a low impurity content, and the purity of pyrite and chalcopyrite was calculated to be 96.38% and 95.05%, respectively.

MFA (Rhawn Chemical Co., Ltd., China) was used as a depressant. Sodium butyl xanthate (NaBX; Rhawn Chemical Co., Ltd., China) was used as a collector. Terpineol oil ($C_{10}H_{17}OH$; Tiefeng Chemical Co., Ltd., China) was used as a foam agent. Sodium chloride (NaCl; Fengchuan Chemical Co., Ltd., China) was used as an electrolyte when performing zeta potential determinations. The stock solutions of sodium hydroxide (NaOH; Fengchuan Chemical Co., Ltd., China) and hydrochloric acid (HCl; Fengchuan Chemical Co., Ltd., China) were prepared to regulate the pH of the solution. All the tests were prepared with deionized (DI) water.

2.2 Flotation experiments

Lab-scale flotation experiment was performed using a mini-type flotation device (effective capacity:

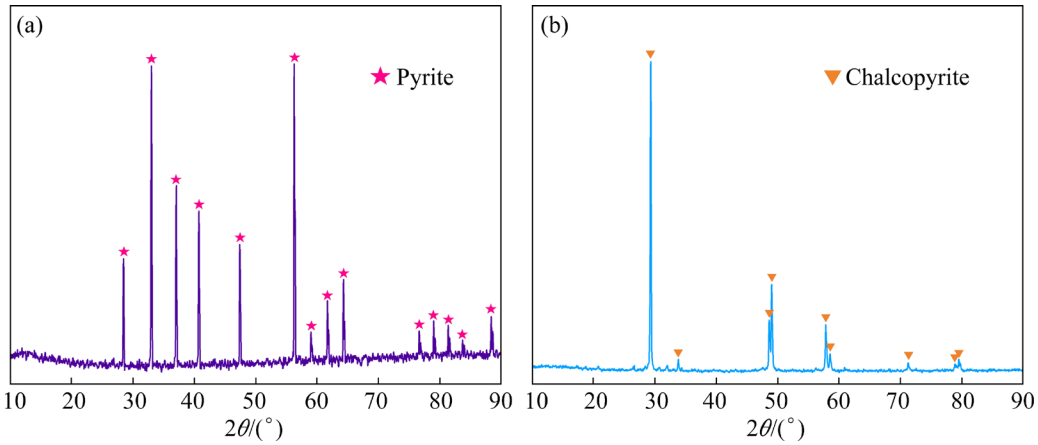

Fig. 1 XRD patterns of pyrite (a) and chalcopyrite (b) specimens

Table 1 Multi-element detection results of chalcopyrite and pyrite specimens (wt.%)

Specimen	Cu	Pb	Zn	S	Fe	CaO	MgO	Al_2O_3	SiO_2
Chalcopyrite	32.85	0.08	0.11	34.66	30.13	0.37	0.19	0.22	0.31
Pyrite	0.03	0.14	0.01	52.09	44.98	0.21	0.14	0.17	0.26

60 mL) supplied by Whrock Co., Ltd., Wuhan, China. The adopted process flow is depicted in Fig. 2.

For single-mineral flotation experiments, 2.0 g of chalcopyrite or pyrite particles were ultrasonically cleaned and transferred to a flotation cell, followed by addition of 40 mL of DI water. After adjusting the pulp pH to be approximately 8.0, the specified dosages of MFA and NaBX solutions were then sequentially added and reacted with the mixture for 5 and 3 min, respectively. Next, terpineol oil was added and reacted with the mixture for 2 min. After completing the reaction, the floated froth products were manually scraped off the liquid surface, and the residual sediments were collected. For mixed-mineral flotation experiments, the pyrite and chalcopyrite particles (mass ratio of 1:1) were mixed as the flotation feed, and the experimental steps and reagent conditions were the same as those described above. The separation efficiency (SE) was calculated based on the following formula:

$$\mathrm{SE}=\frac{(\beta-\alpha)\delta}{(\delta-\alpha)\alpha}\gamma\times100\% \quad (1)$$

where β represents the Cu grade in concentrates, α refers to the Cu grade in flotation feed, δ is the Cu grade (32.85%) of the chalcopyrite tested in this work, and γ denotes the yield of concentrates.

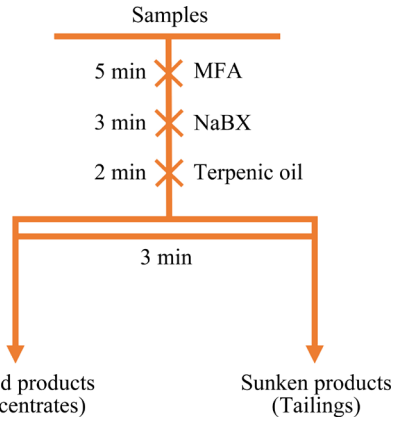

Fig. 2 Process flow adopted in flotation experiments

2.3 Surface adsorption tests

Pyrite and chalcopyrite particles (2.0 g) were separately ultrasonicated and blended with 40 mL of DI water. Subsequently, the mixture was agitated using a magnetic stirrer; MFA and NaBX solutions were then added in sequence and reacted with the mixture for 5 and 3 min, respectively. The reagent concentrations and pulp pH were the same as those used in the flotation experiments. The mixture was allowed to stand for a while after the end of the reaction, and an appropriate portion of the supernatant was then extracted and centrifuged as an aliquot to determine the organic carbon and NaBX contents of the solution using a total organic carbon (TOC) analyzer (Innovox, USA) and an

UV-2700 type spectrometer (Shimadzu, Japan), respectively.

2.4 Zeta potential determination

Mineral particles having a diameter of less than 38 μm were further ground. A 0.1 g portion of the resulting products was then ultrasonically dispersed in a glass beaker containing NaCl solutions (40 mL, 5×10^{-3} mol/L). MFA solutions (150 mg/L) were subsequently added and reacted with the mixture for 5 min. The pH was maintained over the required range throughout the whole reaction process. After this procedure, the mixture was allowed to stand for 5 min. Finally, an appropriate amount of the supernatant was collected and transferred to a mini potential cell to determine the potentials using a 3000HS type zeta analyzer (Malvern Instruments Ltd., UK).

2.5 LEIS tests

The chalcopyrite and pyrite flakes were first inserted in a cylinder (diameter of 3 cm) made of epoxy resin. The resulting flakes were then immersed in KCl solution (1000 mL, 1×10^{-3} mol/L), followed by addition of 150 mg/L MFA solutions. After immersion of the flakes for 5 min, a probe was used to determine the surface impedance of the flakes with the use of a Versa Stat micro-scanning electrochemical test system (VersaSTAT 3F, Ametek, America). It was a three-electrode system in which the Ag/AgCl electrode, mineral flakes, and platinum ring were used as reference, working, and counter electrodes, respectively.

2.6 AFM tests

The pyrite flakes were first cleaned ultrasonically with DI water, after which the cleaned flakes were immersed in a beaker containing 40 mL of 150 mg/L MFA solutions for 5 min (pH=8.0). The resulting flakes were immobilized on a glass sheet after removal of surface moisture from the flakes. The surface topography of the flakes before and after exposure to MFA was imaged with an atomic force microscope (AFM, Bruker Dimension Icon) over a scanned area of 2 μm × 2 μm.

2.7 XPS tests

A 2 g portion of the ultrasonicated pyrite particles was blended with 40 mL of DI water in a beaker. The solution pH was then adjusted to approximately 8.0, and 150 mg/L MFA solutions were introduced and reacted with the particles for 5 min. The resulting pyrite particles were electro-thermally dried in a vacuum oven (25 °C). The XPS spectra of pyrite without and with exposure to MFA were collected using a Versa Probe II type spectrometer (PHI 5000, ULVAC-PHI, Japan).

3 Results and discussion

3.1 Flotation results

Flotation experiments were performed to observe discrepancies in the flotation behavior of pyrite and chalcopyrite with and without the participation of MFA. The flotation results of both minerals with different pulp pH are shown in Fig. 3(a). After subjecting pyrite and chalcopyrite to the NaBX treatment only, the flotation recovery of both minerals was retained at a high level within the pulp pH range of 2−8. However, the flotation recovery of pyrite tended to decrease as the pulp pH was increased to 10, which indicates that a highly alkaline solution environment was unfavorable for the flotation of pyrite. Consequently, subsequent tests were all conducted at a pulp pH of approximately 8.0. Moreover, it was difficult to separate chalcopyrite from pyrite without the use of the depressant in a weak-alkalinity flotation system, because both minerals exhibited excellent floatability after being treated by the collector even at a low dosage. Therefore, MFA was selected as a pyrite depressant to recover chalcopyrite. As shown in Fig. 3(b), the flotation recovery of pyrite rapidly decreased as the concentrations of MFA were increased, and decreased to be less than 10% after addition of MFA at a concentration greater than 150 mg/L. Thus, the floatability of pyrite underwent a considerable change following the pre-treatment with MFA. By contrast, the chalcopyrite recovery slightly reduced for MFA concentrations in the range of 20−200 mg/L, but still reached 86% for the addition of 200 mg/L MFA approximately. These data indicate that MFA markedly inhibited the flotation of pyrite, whereas the flotation of chalcopyrite was only slightly affected. This effect could be attributed to selective adsorption of O-containing hydrophilic functional groups (e.g., Ph—OH or —COOH) on surfaces of pyrite; thus, the floatability of pyrite was markedly attenuated.

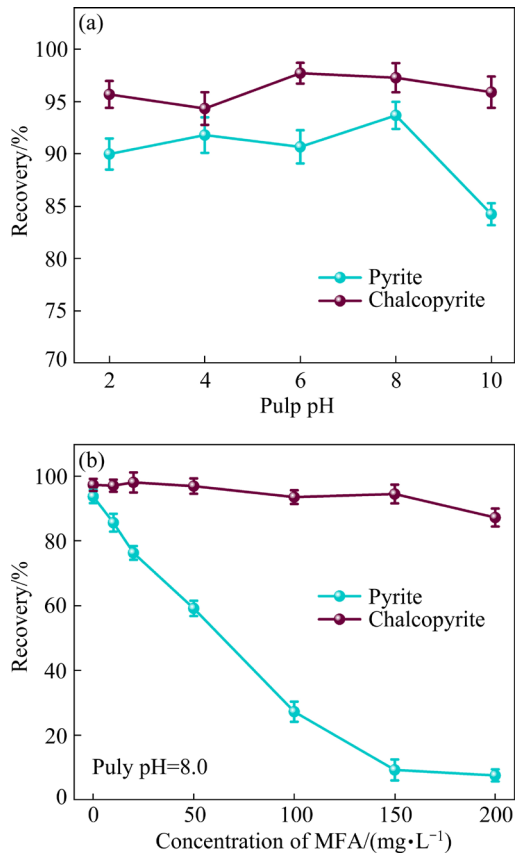

Fig. 3 Flotation recovery of chalcopyrite and pyrite with respect to different pulp pH (a) and MFA concentrations (b) (NaBX=10 mg/L)

The selective inhibition effect of MFA on the pyrite was further examined by testing artificially mixed Cu−Fe sulfide mineral samples. The optimal concentrations of MFA and NaBX were adopted as 150 and 10 mg/L, respectively. The calculated flotation indexes are given in Table 2. The copper recovery in concentrates was 92.26% after exposure of the minerals to NaBX without addition of MFA, whereas the copper grade in concentrates was only 16.01%. Hence, the association of pyrite with chalcopyrite degraded the quality of the copper products. In addition, the separation efficiency was only 3.31% in this case, further confirming the difficulties in separating chalcopyrite from pyrite without a depressant. However, after treating the minerals with MFA and NaBX in sequence, the copper grade in concentrates increased to 28.03%, and copper recovery of 84.79% in concentrates was achieved. Moreover, the separation efficiency increased to 71.66%. These results indicate that even when testing a mixed-mineral sample, the flotation of pyrite was inactivated by MFA whereas that of chalcopyrite was unhindered. Hence, MFA had a favorable selective depression effect on pyrite, and it may have applications as a promising pyrite depressant for effectively recovering chalcopyrite in flotation. On the basis of the flotation results, the associated depression mechanism of MFA on pyrite was characterized by multiple methods.

Table 2 Flotation results of artificially mixed Cu−Fe sulfide minerals

w(MFA)/(mg·L^{-1})	Product	Yield/%	Cu grade/%	Cu recovery/%	SE/%
0	Concentrates	90.55	16.01	92.26	3.31
	Tailings	9.45	12.87	7.74	
	Feed	100.00	15.71	100.00	
150	Concentrates	47.06	28.03	84.79	71.66
	Tailings	52.94	4.47	15.21	
	Feed	100.00	15.56	100.00	

3.2 Surface adsorption analyses

The adsorptive intensity of MFA on both minerals was assessed by performing TOC tests, as shown in Fig. 4(a). After treating pyrite and chalcopyrite with MFA according to concentration used in the flotation experiments, the amounts of residual organic carbon in the pulp increased together with the MFA concentrations. However, the amounts of residual organic carbon in the pulp of MFA-treated pyrite were lower than those of MFA-treated chalcopyrite, indicating that more MFA adsorbed on pyrite than on chalcopyrite. This behavior could account for differential adsorption behaviors of the collector for both minerals.

Accordingly, the ultraviolet−visible spectrophotometry was used to investigate how MFA affected the adsorptive capacity of NaBX on the surfaces of both minerals. As shown in Fig. 4(b), after both minerals were sequentially conditioned with MFA and NaBX, the residual amounts of NaBX in the pulp of MFA-treated pyrite rapidly increased as the MFA concentrations were increased. Conversely, the residual amounts of NaBX in pulp of MFA-treated chalcopyrite slightly fluctuated over the tested MFA concentration range of 20−200 mg/L. These results indicate that MFA exhibited a stronger affinity for pyrite than for chalcopyrite, thus greatly reducing the collector

quantities adsorbed to the pyrite surfaces. The selective adsorption of MFA on pyrite was presumably attributed to the metal ions in the crystals of both chalcopyrite and pyrite, which had different affinities for the organic reagents. This effect contributed to different adsorption performances of the collector on both minerals; hence, the separation of chalcopyrite from pyrite was realized by addition of low concentrations of collector [35,36].

3.3 Zeta potential analyses

Zeta potentials can directly reflect the interactive intensity of floatation agents and minerals [37]. Consequently, the electro-kinetic properties of pyrite and chalcopyrite with and without addition of MFA were assessed from zeta potential determinations. The results presented in Fig. 5 indicate that the potentials of both minerals shifted in a negative direction at a higher pulp pH; thus, more negatively charged OH^- groups were present as the pulp pH was increased. The isoelectric points of pyrite and chalcopyrite were detected at pulp pH of 4.82 and 3.56, respectively, which are in line with previous reports [38,39]. Notably, after both minerals were processed by MFA, the potentials of the MFA-treated pyrite remarkably decreased compared with those of untreated pyrite. Furthermore, the isoelectric point of pyrite greatly shifted. Conversely, the potentials of MFA-treated chalcopyrite were only slightly lowered. These outcomes were attributed to the presence of negatively charged O-containing groups in MFA. These groups selectively adsorbed to the surfaces of pyrite, and induced greater variation in the potentials of pyrite after exposure to MFA. Thus, the zeta potential results are consistent with the behaviors characterized above.

3.4 LEIS analyses

LEIS is a frequency-domain analytical method to accurately measure the impedance parameters of solid and liquid interfaces over micrometer-scale areas [40]. Therefore, this approach was used to investigate the electro-chemical properties of both minerals before and after the treatment with MFA.

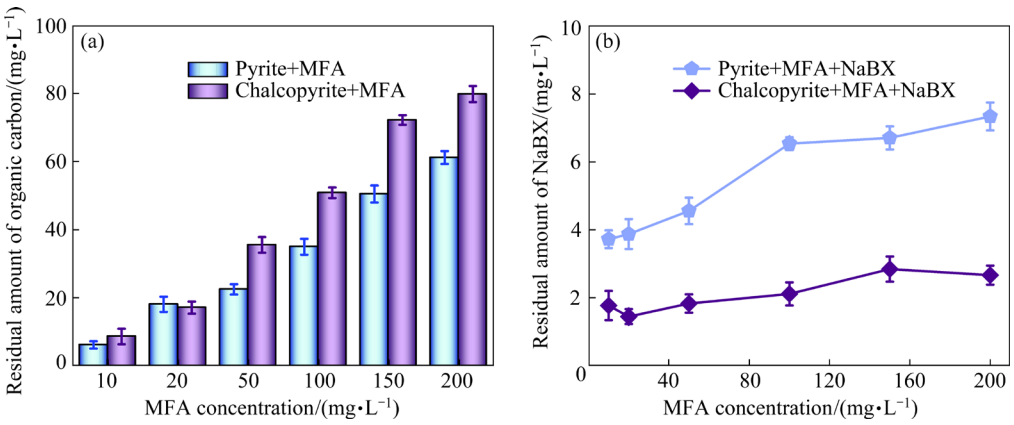

Fig. 4 Residual amounts of organic carbon (a) and NaBX (b) in pulp at various concentrations of MFA (pH=8.0; *w*(NaBX)=10 mg/L)

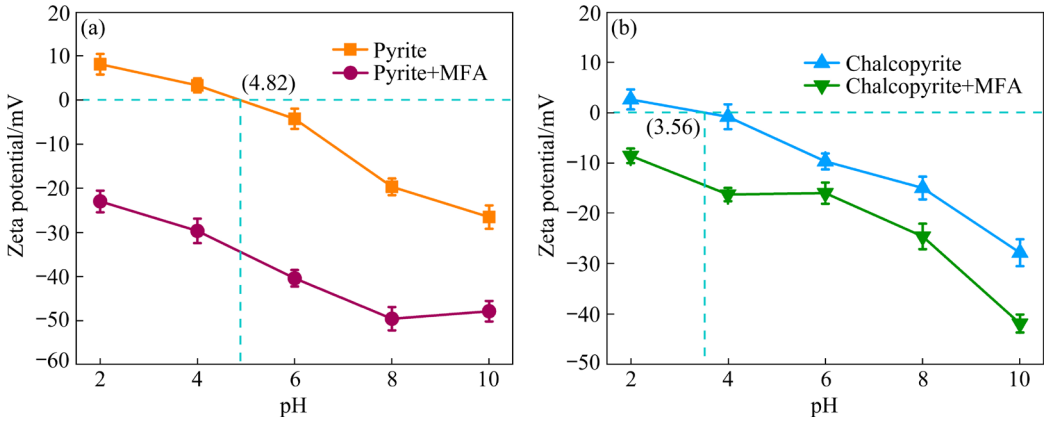

Fig. 5 Zeta potentials of pyrite (a) and chalcopyrite (b) at various pH with and without participation of MFA

The recorded surface impedance diagrams of both minerals are shown in Fig. 6. The average surface impedance of untreated pyrite and chalcopyrite was 117084.83 and 110032.59 Ω, respectively. Next, both minerals were treated by MFA, and the average surface impedance of MFA-treated pyrite and chalcopyrite increased to 119676.28 and 110614.86 Ω, respectively. The results demonstrate the change in the electrochemical properties of both minerals following exposure to MFA. However, the increased extent of the averaged surface impedance of MFA-treated pyrite (2591.45 Ω) was markedly greater than that of MFA-treated chalcopyrite (582.27 Ω), confirming that the adsorptive strength of MFA on pyrite was higher than that on chalcopyrite, thereby having a stronger depression effect on pyrite.

3.5 AFM analyses

The results above confirm that MFA strongly adsorbed to the surfaces of pyrite, which markedly degraded the floatability of pyrite owing to the weakened collector adsorption. According to the aforementioned results, the micro structural features of the surface morphology of MFA-treated pyrite were observed by AFM. The AFM images captured from the surfaces of untreated and MFA-treated pyrite are shown in Fig. 7. R_q and R_a respectively represent the root mean square and average surface roughness. The images of untreated pyrite showed a smooth 2D plane with a uniform 3D cross-sectional morphology. The values of R_q and R_a were 0.65 and 0.50 nm, respectively. These outcomes suggest that untreated pyrite was not contaminated by the impurities. Nevertheless, after subjecting pyrite to the MFA treatment, a rough 2D plane with a non-uniform 3D cross-sectional morphology was presented in the images of MFA-treated pyrite. Moreover, the values of R_a, and R_q increased to 3.12 and 2.08 nm, respectively. These results suggest that the surfaces of pyrite were likely covered by the MFA layers, which increased the surface hydrophilicity of pyrite and impeded the subsequent collector adsorption.

3.6 XPS analyses

The variation in the chemical forms and compositions of the mineral surfaces before and after the treatment with flotation agents can be qualitatively and semi-quantitatively detected by XPS [41]. In this way, the inhibition mechanism of MFA on pyrite was further explored. The survey scans of untreated and MFA-treated pyrite, and the corresponding ratios of target elements are shown in Fig. 8. Pyrite treated with 150 mg/L MFA in a weakly alkaline media showed increased peak intensities of C 1s and O 1s compared with untreated pyrite. Additionally, the proportions of C and O increased from 33.92 and 17.64 at.% to 46.78 and 25.08 at.%, respectively, which indicates that MFA adsorbed to pyrite. Conversely, the intensities of Fe 2p and S 2p peaks markedly decreased, and the proportions of S and Fe decreased from 34.93 and 13.51 at.% to 21.12 and 7.02 at.%, respectively. This result suggests that addition of MFA decreased the amount of hydrophobic S-rich species adsorbed to the surfaces of pyrite, which might be expected to attenuate the floatability of pyrite.

The narrow-range Fe 2p and S 2p spectra were fitted to further reveal the depressive effect of MFA on pyrite, as represented in Figs. 9 and 10. The corresponding ratios of Fe-based and S-based species are summarized in Tables 3 and 4. As shown in Fig. 9, the Fe 2p spectra of untreated and MFA-treated pyrite were fitted by three singlet peaks, wherein the peaks fitted at 707.42 and 707.50 eV corresponded to Fe(II)—S species, those at 709.08 and 709.63 eV corresponded to Fe—O species, and those at 711.06 and 711.63 eV corresponded to Fe(III)—OOH species [42−44]. For untreated pyrite, the proportions of Fe(II)—S, Fe—O, and Fe(III)—OOH species among all Fe-based species were calculated to be 77.38%, 12.85% and 9.77%, respectively. Nevertheless, after pyrite was exposed to 150 mg/L MFA at a pulp pH of 8.0, the ratio of Fe(II)—S species decreased to 68.45%, whereas the ratios of Fe—O and Fe(III)—OOH species increased to 15.11% and 16.44%, respectively. The depressed flotation of pyrite by MFA was confirmed from the increased quantities of Fe—O and Fe(III)—OOH species, because these species are hydrophilic in nature and unfavorable for the flotation of pyrite. Moreover, compared with the untreated pyrite, MFA-treated pyrite featured binding energies of Fe—O and Fe(III)—OOH species that were positively shifted by 0.57 and 0.55 eV, respectively. These data suggest that the presence of MFA significantly altered the chemical states of Fe-based species, further confirming the strong adsorption to the pyrite surfaces.

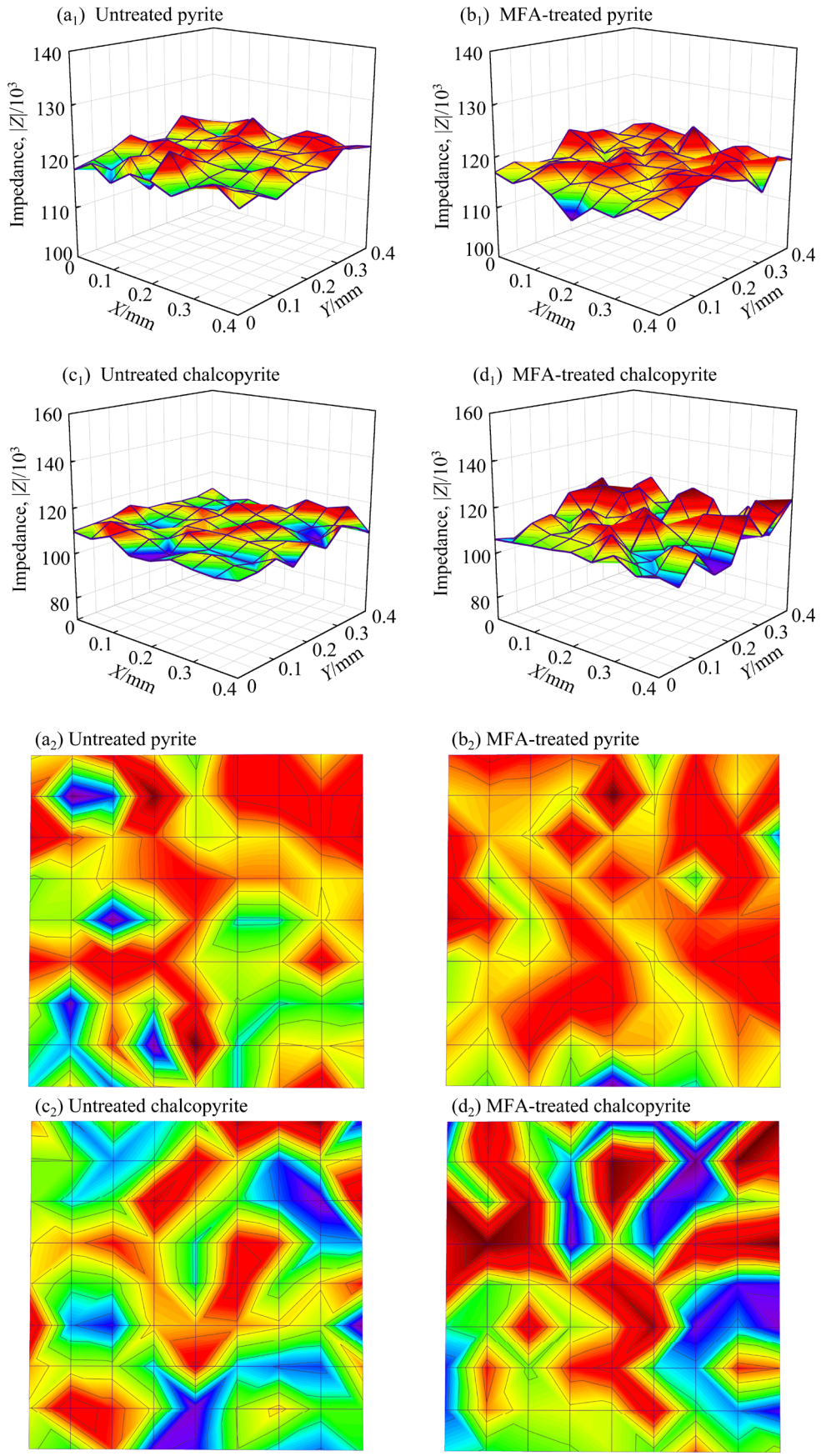

Fig. 6 LEIS images detected from surfaces of pyrite and chalcopyrite without and with participation of MFA (Scanning area: 0.40 mm × 0.40 mm): (a_1−d_1) Side views; (a_2−d_2) Top views

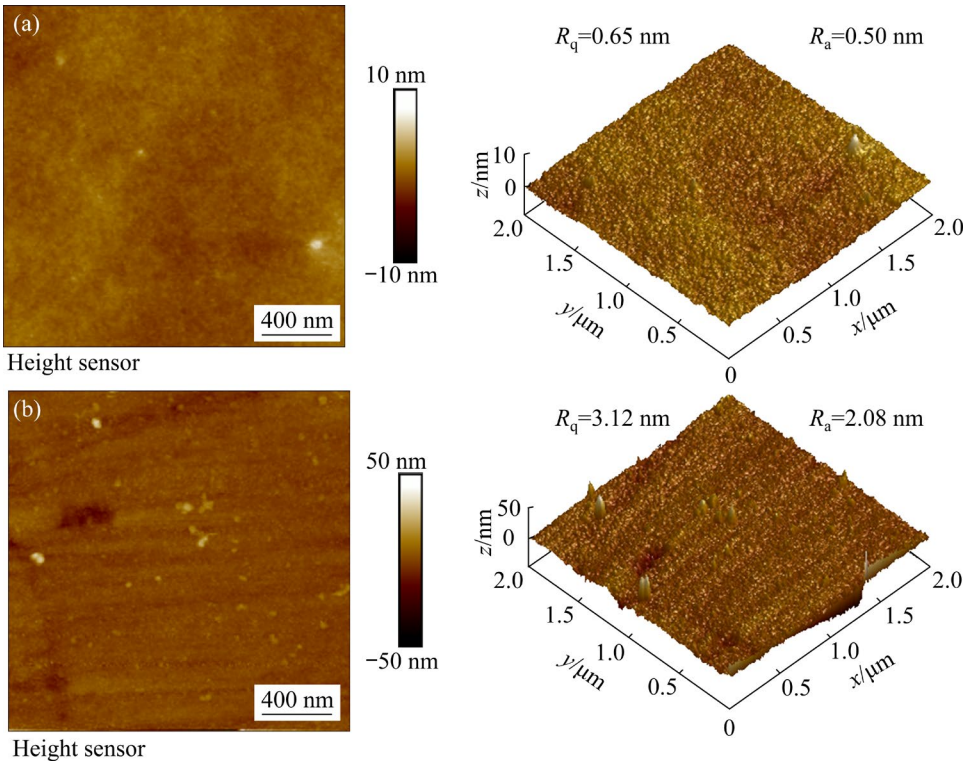

Fig. 7 AFM images detected from surfaces of untreated (a) and MFA-treated pyrite (b)

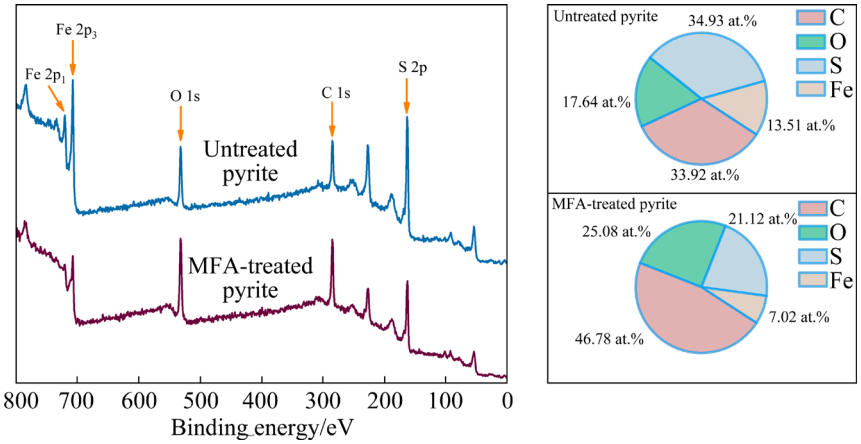

Fig. 8 Full-scan XPS spectra of pyrite before and after exposure to MFA and corresponding elemental contents

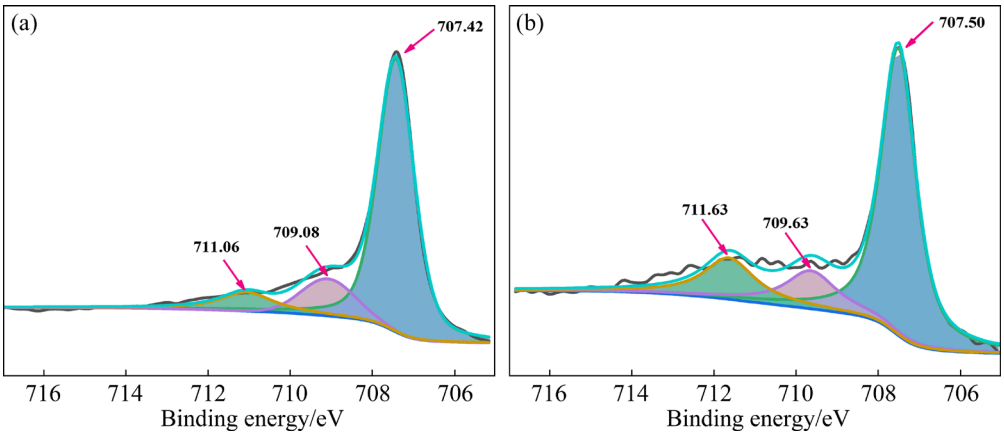

Fig. 9 Fitted narrow-scan Fe 2p spectra detected from surfaces of untreated (a) and MFA-treated (b) pyrite

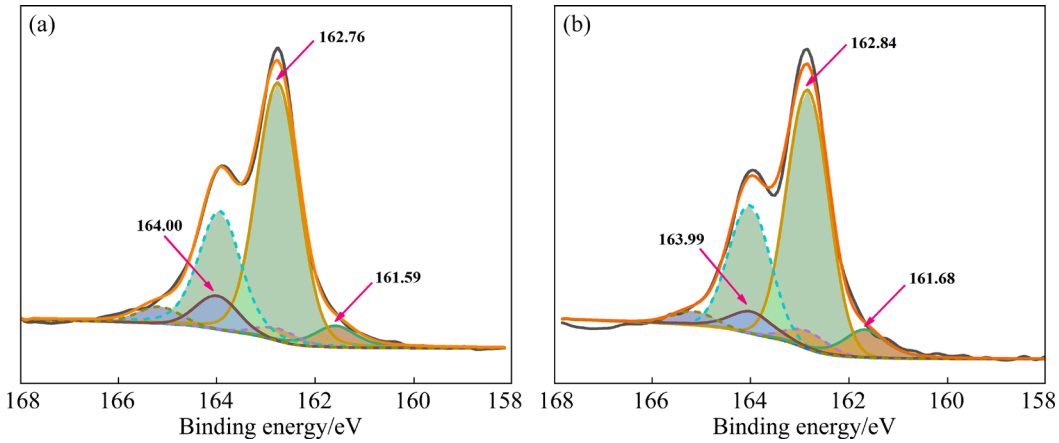

Fig. 10 Fitted narrow-scan S 2p spectra detected from surfaces of untreated (a) and MFA-treated (b) pyrite

Table 3 Binding energy and calculated ratios of Fe-based species on surfaces of untreated and MFA-treated pyrite

Specimen	Binding energy/eV			Ratio/%		
	Fe(II)—S	Fe—O	Fe(III)—OOH	Fe(II)—S	Fe—O	Fe(III)—OOH
Untreated pyrite	707.42	709.08	711.06	77.38	12.85	9.77
MFA-treated pyrite	707.50	709.63	711.63	68.45	15.11	16.44

Table 4 Binding energy and calculated ratios of S-based species on surfaces of untreated and MFA-treated pyrite

Specimen	Binding energy/eV			Ratio/%		
	S^{2-}	S_2^{2-}	S_n^{2-}	S^{2-}	S_2^{2-}	S_n^{2-}
Untreated pyrite	161.59	162.76	164.00	7.97	82.00	10.03
MFA-treated pyrite	161.68	162.84	163.99	11.10	80.37	8.53

The S 2p spectra of untreated and MFA-treated pyrite (Fig. 10) were fitted by three groups of symmetrical peaks, wherein the peaks at 161.59 and 161.68 eV were assigned to S^{2-} species, those at 162.76 and 162.84 eV were attributed to S_2^{2-} species, and those at 164.00 and 163.99 eV corresponded to S_n^{2-} species [42,45,46]. After treating pyrite with MFA, the ratio of S^{2-} species increased from 7.97% to 11.10%, whereas the ratios of S_2^{2-} and S_n^{2-} species decreased from 82.00% and 10.03% to 80.37% and 8.53%, respectively. Notably, the floatability of pyrite is related to the reactivity and amounts of S_2^{2-} and S_n^{2-} species [42]. A slight variation occurred in the binding energies of S-based species on the pyrite surfaces before and after the treatment with MFA. However, in combination with the analysis results for the fitted Fe 2p spectra, it can be deduced that the presence of MFA facilitated the formation and adsorption of hydrophilic species to the pyrite surfaces.

4 Potential depression mechanism

On the basis of these analysis results, a schematic diagram (Fig. 11) was plotted to describe how MFA degraded the surface hydrophobicity of pyrite during the flotation of chalcopyrite in a weakly alkaline pulp system. A larger amount of MFA was adsorbed to pyrite than to chalcopyrite after exposure of both minerals to MFA. This effect could result from the selective adsorption of hydrophilic groups in MFA to the pyrite surfaces, which would be expected to generate more hydrophilic species. This behavior would detrimentally affect the subsequent interactions of collector with pyrite, thus contributing to a reduction in the floatability of pyrite. Conversely, chalcopyrite was only slightly affected by MFA and effectively floated even at a higher dose of MFA, consequently realizing separation of chalcopyrite

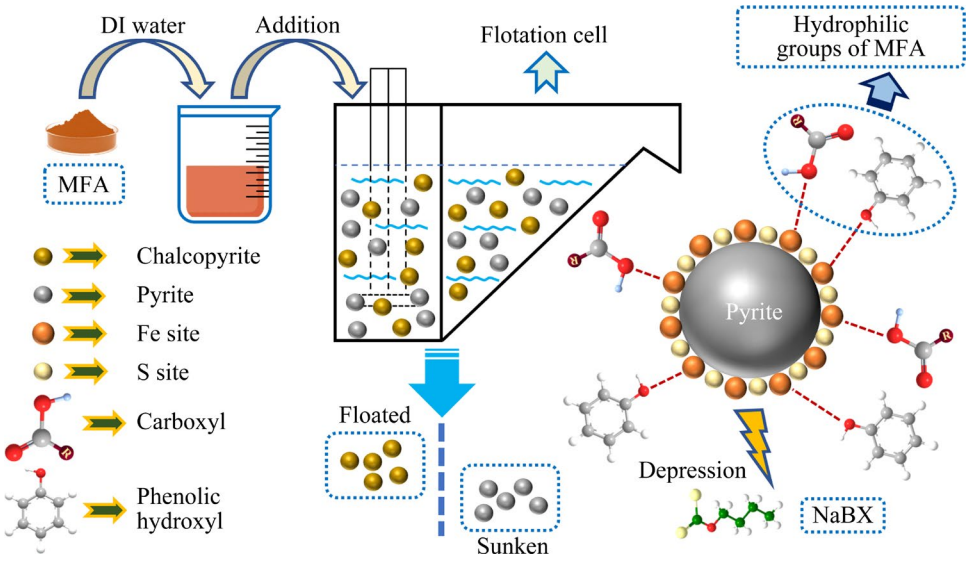

Fig. 11 Schematic diagram of selective depressing effect of MFA on pyrite for floating chalcopyrite in weak-alkalinity solution system

from pyrite. This work reveals that MFA is a promising alternative pyrite depressant for beneficiating chalcopyrite and other target minerals.

5 Conclusions

(1) The flotation of pyrite was markedly inhibited by MFA whereas that of chalcopyrite was only slightly hindered even at a high concentration of MFA. This behavior facilitated the separation of chalcopyrite and pyrite by addition of 150 mg/L MFA at a solution pH of nearly 8.0.

(2) The adsorption of MFA on pyrite was stronger than that on chalcopyrite, inhibiting the adsorption of subsequently added collector on pyrite; thus, the hydrophobicity of pyrite was attenuated.

(3) The surfaces of pyrite were covered by the MFA layers after being exposed to MFA. Additionally, more hydrophilic Fe-based species were generated. Hence, these effects degraded the floatability of pyrite.

CRediT authorship contribution statement

Zhi-hao SHEN: Investigation, Data curation, Formal analysis, Methodology, Software, Writing – Original draft, Writing – Review & editing; **Shu-ming WEN:** Investigation, Methodology, Project administration, Resources, Supervision, Validation, Writing – Review & editing; **Jia-mei HAO:** Investigation, Methodology, Validation, Writing – Review & editing; **Qi-cheng FENG:** Conceptualization, Funding acquisition, Investigation, Methodology, Project administration, Validation, Writing – Review & editing.

Declaration of competing interest

The authors declare that they have no known competing financial interests or personal relationships that could have appeared to influence the work reported in this paper.

Acknowledgments

This work was supported by Fundamental Research Projects of Yunnan Province, China (Nos. 202101BE070001-009, 202301AU070189).

References

[1] FENG Qi-cheng, YANG Wen-hang, WEN Shu-ming, WANG Han, ZHAO Wen-juan, HAN Guang. Flotation of copper oxide minerals: A review [J]. International Journal of Mining Science and Technology, 2022, 32(6): 1351−1364.

[2] LI Li-quan, PAN De-an, LI Bin, WU Yu-feng, WANG Huai-dong, GU Yi-fan, ZUO Tie-yong. Patterns and challenges in the copper industry in China [J]. Resources, Conservation and Recycling, 2017, 127: 1−7.

[3] LIAO Run-peng, HU Pan-jin, WEN Shu-ming, ZHENG Yong-xing, QIU Xian-hui, LÜ Jin-fang, LIU Jian. Interaction mechanism of ferrate(VI) with arsenopyrite surface and its effect on flotation separation of chalcopyrite from arsenopyrite [J]. Transactions of Nonferrous Metals Society of China, 2022, 32(11): 3731−3743.

[4] HAO Jia-mei, LIU Jian, YU Yun-long, GAO Hu-lin, QIN Xiao-yan, BAI Xu. Depressants for separation of chalcopyrite and molybdenite: Review and prospects [J]. Minerals Engineering, 2023, 201: 108209.

[5] BAI Yun-long, WANG Wei, XIE Feng, LU Dian-kun, JIANG Kai-xi. Effect of temperature, oxygen partial pressure and calcium lignosulphonate on chalcopyrite dissolution in sulfuric acid solution [J]. Transactions of Nonferrous Metals Society of China, 2022, 32(5): 1650−1663.

[6] HE Hai-yang, FANG Jian-jun, QIU Zhi-lian, LIU Dian-wen, XIE Hai-yun, SHEN Pei-lun, PENG Rong, PENG Li-guo, QIN Shuang, DONG Shi-qin. Selective galena depression mechanism of tea polyphenol in chalcopyrite flotation [J]. Minerals Engineering, 2023, 202: 108259.

[7] KHOSO S A, HU Yue-hua, LYU Fei, Liu Run-qing, SUN Wei. Selective separation of chalcopyrite from pyrite with a novel non-hazardous biodegradable depressant [J]. Journal of Cleaner Production, 2019, 232: 888−897.

[8] BU Xian-zhong, FENG Yuan-yuan, XUE Ji-wei, YANG Lu, ZHANG Chong-hui. Effective recovery of chalcopyrite at low temperatures using modified ester collector [J]. Transactions of Nonferrous Metals Society of China, 2022, 32(1): 296−306.

[9] HAN Guang, WEN Shu-ming, WANG Han, FENG Qi-cheng. Interaction mechanism of tannic acid with pyrite surfaces and its response to flotation separation of chalcopyrite from pyrite in a low-alkaline medium [J]. Journal of Materials Research and Technology, 2020, 9(3): 4421−4430.

[10] ZHANG Ye, LIU Run-qing, SUN Wei, Wang Li, DONG Yan-hong, WANG Chang-tao. Electrochemical mechanism and flotation of chalcopyrite and galena in the presence of sodium silicate and sodium sulfite [J]. Transactions of Nonferrous Metals Society of China, 2020, 30(4): 1091−1101.

[11] CAO Zhao, CHEN Xu-meng, PENG Yong-jun. The role of sodium sulfide in the flotation of pyrite depressed in chalcopyrite flotation [J]. Minerals Engineering, 2018, 119: 93−98.

[12] MURPHY R, STRONGIN D R. Surface reactivity of pyrite and related sulfides [J]. Surface Science Reports, 2009, 64(1): 1−45.

[13] MOSLEMI H, GHARABAGHI M. A review on electrochemical behavior of pyrite in the froth flotation process [J]. Journal of Industrial and Engineering Chemistry, 2017, 47: 1−18.

[14] CAO Zhao, WANG Peng, ZHANG Wen-bo, ZENG Xiao-bo, CAO Yong-dan. Mechanism of sodium sulfide on flotation of cyanide-depressed pyrite [J]. Transactions of Nonferrous Metals Society of China, 2020, 30(2): 484−491.

[15] LUO S, MCCLELLAND J F, WHEELOCK T D. The interaction of thioglycolic acid and pyrite [J]. Coal Science and Technology, 1993, 21: 55−69.

[16] ZHAO Cui-hua, HUANG De-wei, CHEN Jian-hua, LI Yu-qiong. CHEN Ye, LI Wei-zhou. The interaction of cyanide with pyrite, marcasite and pyrrhotite [J]. Minerals Engineering, 2016, 95: 131−137.

[17] GUO Bao, PENG Yong-jun, PARKER G. Electrochemical and spectroscopic studies of pyrite–cyanide interactions in relation to the depression of pyrite flotation [J]. Minerals Engineering, 2016, 92: 78−85.

[18] HAN Guang, WEN Shu-ming, WANG Han, FENG Qi-cheng. Lactic acid as selective depressant for flotation separation of chalcopyrite from pyrite and its depression mechanism [J]. Journal of Molecular Liquids, 2019, 296: 111774.

[19] MU Yu-fan, PENG Yong-jun, LAUTEN R A. The depression of pyrite in selective flotation by different reagent systems—A Literature review [J]. Minerals Engineering, 2016, 96/97: 143−156.

[20] HAN Guang, WEN Shu-ming, WANG Han, FENG Qi-cheng. Effect of starch on surface properties of pyrite and chalcopyrite and its response to flotation separation at low alkalinity [J]. Minerals Engineering, 2019, 143: 106015.

[21] LIU Run-qing, SUN Wei, Hu Yue-hua, WANG Dian-zuo. Effect of organic depressant lignosulfonate calcium on separation of chalcopyrite from pyrite [J]. Journal of Central South University, 2009, 16: 0753−0757.

[22] MU Yu-fan, PENG Yong-jun, LAUTEN R A. Electrochemistry aspects of pyrite in the presence of potassium amyl xanthate and a lignosulfonate-based biopolymer depressant [J]. Electrochimica Acta, 2015, 174: 133−142.

[23] BICAK O, EKMEKCI Z, BRADSHAW D J, HARRIS P J. Adsorption of guar gum and CMC on pyrite [J]. Minerals Engineering, 2007, 20: 996−1002.

[24] LIU Qi, ZHANG Ya-hui, LASKOWSKI J S. The adsorption of polysaccharides onto mineral surfaces: an acid/base interaction [J]. International Journal of Mineral Processing, 2000, 60(3/4): 229−245.

[25] HUANG Peng, CAO Ming-li, LIU Qiu. Selective depression of pyrite with chitosan in Pb−Fe sulfide flotation [J]. Minerals Engineering, 2013, 46/47: 45−51.

[26] HAN Guang, WEN Shu-ming, WANG Han, FENG Qi-cheng. Selective adsorption mechanism of salicylic acid on pyrite surfaces and its application in flotation separation of chalcopyrite from pyrite [J]. Separation and Purification Technology, 2020, 240: 116650.

[27] HAN Guang, WEN Shu-ming, WANG Han, FENG Qi-cheng, BAI Xu. Pyrogallic acid as depressant for flotation separation of pyrite from chalcopyrite under low-alkalinity conditions [J]. Separation and Purification Technology, 2021, 267: 118670.

[28] LIU De-zhi, ZHANG Guo-fan, CHEN Yan-fei, HUANG Gang-hong, GAO Ya-wen. Investigations on the utilization of konjac glucomannan in the flotation separation of chalcopyrite from pyrite [J]. Minerals Engineering, 2020, 145: 106098.

[29] BAI Xu, LIU Jian, WEN Shu-ming, LIN Yi-lin. Selective separation of chalcopyrite and pyrite using a novel organic depressant at low alkalinity [J]. Minerals Engineering, 2022, 185: 107677.

[30] BAI Xu, LIU Jian, WEN Shu-ming, LIN Yi-lin. Effect and mechanism of organic depressant on the hydrophobicity of chalcopyrite and pyrite under weakly alkaline environment [J]. Journal of Materials Research and Technology, 2021, 15: 4109−4116.

[31] KARTHE S, SZARGAN R, SUONINEN E. Oxidation of pyrite surfaces: A photoelectron spectroscopic study [J]. Applied Surface Science, 1993, 72(2): 157−170.

[32] WANG Zhen, QIAN Yun-lou, XU Long-hua, DAI Bo, XIAO Jun-hui, Fu Kai-bin. Selective chalcopyrite flotation from pyrite with glycerine−xanthate as depressant [J]. Minerals Engineering, 2015, 74: 86−90.

[33] TANG Wang-wang, ZENG Guang-ming, GONG Gi-lai, LIANG Jie, XU Piao, ZHANG Chang, HUANG Bin-bin. Impact of humic/fulvic acid on the removal of heavy metals from aqueous solutions using nanomaterials: A review [J]. Science of the Total Environment, 2014, 468/469: 1014−1027.

[34] ISLAM M A, MORTON D W, JOHNSON B B, ANGOVE M J. Adsorption of humic and fulvic acids onto a range of adsorbents in aqueous systems, and their effect on the adsorption of other species: A review [J]. Separation and Purification Technology, 2020, 247: 116949.

[35] ZHANG Xing-rong, QIAN Zhi-bo, ZHENG Gui-bing, ZHU Yang-ge, WU Wei-guo. The design of a macromolecular depressant for galena based on DFT studies and its application [J]. Minerals Engineering, 2017, 112: 50−56.

[36] ZHANG X R, ZHU Y G, ZHENG G B, HAN L, MCFADZEAN B, QIAN Z B, PIAO Y C, O'CONNOR C. An investigation into the selective separation and adsorption mechanism of a macromolecular depressant in the galena–chalcopyrite system [J]. Minerals Engineering, 2019, 134: 291−299.

[37] FENG Qi-cheng, WANG Mei-li, ZHANG Ga, ZHAO Wen-juan, HAN Guang. Enhanced adsorption of sulfide and xanthate on smithsonite surfaces by lead activation and implications for flotation intensification [J]. Separation and Purification Technology, 2023, 307: 122772.

[38] QIU Xian-hui, HUANG Zhi-jun, CAO Fei, SUN De-si, WANG Pingping, CHEN Chao-fang. Flotation separation of chalcopyrite from pyrite using a novel *O*-n-butyl-N-isobutyl thionocarbamate as the selective collector [J]. Colloids and Surfaces A: Physicochemical and Engineering Aspects, 2023, 661: 130890.

[39] ZHANG Hong-liang, ZHANG Feng, SUN Wei, CHEN Dai-xiong, CHEN Jian-hua, WANG Rong, HAN Ming-jun, ZHANG Chen-yang. The effects of hydroxyl on selective separation of chalcopyrite from pyrite: A mechanism study [J]. Applied Surface Science, 2023, 608: 154963.

[40] LIU Deng-cheng, LIN Rui, FENG Bo-wen, HAN Li-hang, ZHANG Yu, NI Meng, WU Sai. Localised electrochemical impedance spectroscopy investigation of polymer electrolyte membrane fuel cells using Print circuit board based interference-free system [J]. Applied Energy, 2019, 254: 113712.

[41] LU Wan-ming, WEN Shu-ming, LIU Dian-wen, WANG Han, FENG Qi-cheng. A novel method for improving sulfidization xanthate flotation of malachite: Copper–ammonium synergistic activation [J]. Applied Surface Science, 2023, 618: 156660.

[42] DING Zhan, BI Yun-xiao, LI Jie, YUAN Jia-qiao, DAI Hui-xin, BAI Shao-jun. Flotation separation of chalcopyrite and pyrite via Fenton oxidation modification in a low alkaline acid mine drainage (AMD) system [J]. Minerals Engineering, 2022, 187: 107818.

[43] NESBITT H W, MUIR I J. X-ray photoelectron spectroscopic study of a pristine pyrite surface reacted with water vapor and air [J]. Geochimica et Cosmochimica Acta, 1994, 58: 4667−4679.

[44] FAIRTHORNE G, FORNASIERO D, RALSTON J. Effect of oxidation on the collectorless flotation of chalcopyrite [J]. International Journal of Mineral Processing, 1997, 49: 31−48.

[45] KANTAR C, ORAL O, URKEN O, OZ N A, KESKIN S. Oxidative degradation of chlorophenolic compounds with pyrite−Fenton process [J]. Environmental Pollution, 2019, 247: 349−361.

[46] CAI Yuan-fei, PAN Yu-guan, XUE Ji-yue, SUN Qing-feng, SU Gui-zhen, LI Xiang. Comparative XPS study between experimentally and naturally weathered pyrites [J] Applied Surface Science, 2009, 255: 8750−8760.

矿源黄腐酸作为选择性抑制剂在弱碱性条件下浮选分离黄铜矿和黄铁矿

沈智豪，文书明，郝佳美，丰奇成

昆明理工大学 国土资源工程学院 省部共建复杂有色金属资源清洁利用国家重点实验室，昆明 650093

摘　要：以矿源黄腐酸(MFA)作为环保型黄铁矿抑制剂，以丁基黄药作为捕收剂对黄铜矿进行了浮选回收。浮选实验表明，MFA 对黄铁矿的抑制作用要强于黄铜矿，并在矿浆 pH 约为 8.0 且添加 150 mg/L MFA 的条件下实现了黄铜矿和黄铁矿的浮选分离。其中，铜品位、铜回收率和分离效率分别为 28.03%、84.79%和 71.66%。表面吸附实验、zeta 电位测定以及局部电化学阻抗测试表明，MFA 在黄铁矿表面的吸附量要多于在黄铜矿表面的吸附量，这削弱了捕收剂和黄铁矿之间的相互作用。此外，原子力显微镜成像进一步证实了 MFA 在黄铁矿上的吸附，且 X 射线光电子能谱结果表明黄铁矿在与 MFA 相互作用后其表面的亲水性含铁组分有所增加，从而削弱了自身的可浮性。

关键词：矿源黄腐酸；黄铜矿；黄铁矿；浮选分离

(Edited by Bing YANG)